Cancer Immunol Immunother (2006) 55: 785–796
DOI 10.1007/s00262-005-0082-x

ORIGINAL ARTICLE

Bernd Schlereth · Petra Kleindienst · Iduna Fichtner
Grit Lorenczewski · Klaus Brischwein
Sandra Lippold · Antonio da Silva · Mathias Locher
Roman Kischel · Ralf Lutterbüse · Peter Kufer
Patrick A. Baeuerle

Potent inhibition of local and disseminated tumor growth in immunocompetent mouse models by a bispecific antibody construct specific for Murine CD3

Received: 17 May 2005 / Accepted: 10 August 2005 / Published online: 27 September 2005

Abstract Bispecific single-chain antibody constructs specific for human CD3 have been extensively studied for antitumor activity in human xenograft models using severe combined immunodeficient mice supplemented with human T cells. High efficacy at low effector-to-target ratios, independence of T cell costimuli and a potent activation of previously unstimulated polyclonal T cells were identified as hallmarks of this class of bispecific antibodies. Here we studied a bispecific single-chain antibody construct (referred to as 'bispecific T cell engager', BiTE) in an immunocompetent mouse model. This was possible by the use of a murine CD3-specific BiTE, and a syngeneic melanoma cell line (B16F10) expressing the human Ep-CAM target. The murine CD3-specific BiTE, called 2C11x4-7 prevented in a dose-dependent fashion the outgrowth of subcutaneously growing B16/Ep-CAM tumors with daily i.v. injections of 5 or 50 μg BiTE which was most effective. Treatment with 2C11x4-7 was effective even when it was started 10 days after tumor cell inoculation but delayed treatments showed a reduction in the number of cured animals. 2C11x4-7 was also highly active in a lung tumor colony model. When treatment was started on the day of intravenous tumor cell injection, seven out of eight animals stayed free of lung tumors, and three out of eight animals when treatment was started on day 5. Our study shows that BiTEs also have a high antitumor activity in immunocompetent mice and that there is no obvious need for costimulation of T cells by secondary agents.

Keywords Ep-CAM · Bispecific antibody · Xenograft model · T lymphocyte · Tumor immunity

Bernd Schlereth and Petra Kleindienst contributed equally to this work.

B. Schlereth (✉) · P. Kleindienst · G. Lorenczewski
K. Brischwein · S. Lippold · A. da Silva · M. Locher
R. Kischel · R. Lutterbüse · P. Kufer · P. A. Baeuerle
Micromet AG, Staffelseestr 2, 81477 Munich, Germany
E-mail: bernd.schlereth@micromet.de
Tel.: +49-89-895277502
Fax: +49-89-895277505

I. Fichtner
Experimental Pharmacology and Oncology (EPO),
13122 Berlin-Buch, Germany

Introduction

The concept of treating malignant diseases with bispecific antibodies recruiting T cells dates back to 1985 [1, 2]. To date, bispecific antibody formats that are still actively pursued in preclinical and early clinical development include diabodies, tandem diabodies, cross-linked *F*(ab) fragments, trispecific quadroma antibodies and tandem single-chain antibodies [3]. For clinical use, bispecific antibodies have to be stable and highly active proteins that can be easily manufactured in large quantities. Many attempts have been made but few formats fulfilled all specifications and finally progressed to clinical trials [4, 5].

One subclass of bispecific single-chain antibody constructs appears to meet most requirements for the development of therapeutic bispecific antibodies. This subclass referred to as 'bispecific T cell engager' (BiTE) recognizes with one arm the epsilon subunit of the CD3 complex present on all T cells [5]. With the other single-chain antibody arm, BiTEs can target, for instance, a differentially expressed tumor-associated cell surface antigen. BiTEs are non-glycosylated, monomeric polypeptides of 55,000–60,000 daltons molecular weight. Particularly well studied is bscCD19xCD3, a BiTE molecule directed against the CD19 antigen present on B cells and most B cell malignancies [6–11]. BscCD19×CD3 can initiate redirected target cell lysis by T cells in vitro at low picomolar to femtomolar concentrations, is effective at very low effector-to-target cell

ratios, and does not require costimuli for potent activation of resting peripheral T cells [6]. BiTE-activated human T cells can also eliminate MHC class I-negative tumor cells [12], which may escape immune surveillance by T cells, as well as rodent cells expressing the human target antigen [13]. BiTEs do show an exquisite specificity. Although monomeric BiTEs can bind to T cells, these are only activated in the presence of target cells, suggesting that a polyvalent BiTE matrix on target cells is necessary for T cell activation. Since the activation of T cells by BiTEs is polyclonal, a large effector cell population is available for redirected lysis. BiTEs not only induce target cell lysis, but also trigger secretion of pro-inflammatory cytokines and T cell proliferation, potentially promoting activation and proliferation of tumor-resident effector T cells.

Here, we report on the construction and characterization of two new BiTE molecules named diL2Kx4-7 and 2C11x4-7, both of which are specific for human Ep-CAM (epithelial cell adhesion molecule) and share the same Ep-CAM binding arm. The other binding arm of diL2Kx4-7 is specific for human CD3, whereas for 2C11x4-7, it is specific for murine CD3. Ep-CAM was selected as BiTE target because it is expressed at very high levels on the surface of most carcinomas, including breast, ovary, colon, prostate and lung cancers [14, 15]. Ep-CAM is also targeted by a number of other bispecific antibody formats [16, 17], as well as by murine and humanized monoclonal antibody therapies [18–20].

DiL2K×4-7 with its specificity for human CD3 can only be analyzed for its in vivo efficacy in human xenograft models, e.g. non-obese diabetes/severe combined immunodeficiency disease (NOD/SCID) mice engrafted with human T and tumor cells. To explore the antitumor activity of Ep–CAM-specific BiTE molecules, we generated a BiTE (2C11x4-7) with specificity for murine CD3 that can be tested in immunocompetent mouse models. Here, we show that 2C11×4–7 has comparable in vitro and in vivo biological activity as the human-specific BiTE molecule diL2Kx4-7. Most importantly, we demonstrate that BiTEs also have high antitumor activity in immunocompetent mouse models against both local and disseminated syngeneic tumors.

Materials and methods

Cell lines

NALM-6 B-lymphoma cells were purchased from the 'Deutsche Sammlung von Mikroorganismen und Zelllinien' (DSMZ, Braunschweig, Germany) and transfected with human Ep-CAM cDNA. Kato III, DHFR deficient CHO cells and B16F10 cells were purchased from the American Type Cell Culture Collection (ATCC, Manassas, USA). The Ep-CAM transfected B16F10 cell line (B16F10/Ep-CAM) was kindly provided by Dr. P. Björk (Active Biotech, Lund, Sweden). The number of Ep-CAM binding sites on B16F10/Ep-CAM cells was determined by the BIOCYTEX (QIFIKIT, DakoCytomation, Denmark) kit according to the manufacturer's instructions [21] [22]. Briefly, subconfluent cells were trypsinized, washed and 5×10^4 cells per well added to a 96-well plate in duplicate. After centrifugation of culture plates at 300g for 5 min, cells were re-suspended in 50 µl of a threefold serial dilution of primary antibody in FACS buffer and incubated at 2–8°C for 45 min. To quantify target expression levels, cells and calibration beads were re-suspended in 100 µl of the appropriate secondary antibody. After incubation at 2–8°C for 45 min, samples were washed three times and re-suspended in 200 µl of FACS buffer. Surface staining of cells was analyzed by flow cytometry using a FacsCalibur instrument (Becton Dickinson, Heidelberg, Germany). The number of surface binding sites was determined from the bead calibration curve. Nonlinear regression analysis of equilibrium binding curves was done with GraphPad Prism version 3.0 (GraphPad Software, San Diego, CA).

Kato III cells were cultured in RPMI, 10% FCS; DHFR deficient CHO cells were cultured in MEM-α medium with nucleosides (10 µg/ml, Sigma, Taufkirchen, Germany) and 10% FCS; Nalm-6/Ep-CAM cells were cultured in RPMI 1640, 10% FCS, 3 mg/ml G418; B16F10 cells were cultured in DMEM, 10% FCS and B16F10/Ep-CAM were cultured in RPMI 1640, 10% FCS, 1 mg/ml G418.

BiTE construction and production

DiL2Kx4-7 and 2C11x4-7 were engineered by recombinant DNA technology using the 4–7 single-chain antibody specific for human Ep-CAM [23] as well as the diL2K single-chain antibody specific for human CD3 and the hamster anti-mouse CD3ε antibody 145 2C11 specific for murine CD3 [24], respectively. The diL2K single-chain antibody was derived from the human CD3-specific single-chain antibody L2K via deimmunization (Biovation, Aberdeen, UK). The coding sequences of the diL2K and 2C11 single-chain antibodies were modified via PCR to allow for cloning in front of the coding sequence of the 4–7 single-chain antibody in the eukaryotic expression vector pEFDHFR [23]. The primer sets (5′diL2K: AGGTGTACACTCCGACGTCCAACTG GTGCAGTCAG; 3′diL2K: AATCCGGATTTGA-TCTCCACCTTGGTCCCG; 5′2C11: GGTGTACAC TCCGATTACAAGGACGACGATGACAAGGAGG TGCAGCTGGTGGAG; 3′2C11: GGATCCGGAC CGTTTGATTTCCAGCTTGGTGC) were used to create 5′ flanking BsrGI sites and 3′ flanking BspEI sites as well as 5′ Flag or His tags. The amplified sequences were cloned into the pEFDHFR vector containing a eukaryotic leader peptide sequence [25]. The coding sequence of the inserts was verified by sequencing according to standard protocols [26] and the expression plasmids transfected into DHFR deficient CHO cells. Eukaryotic protein expression in DHFR deficient CHO

cells was performed according to Kaufman et al. [27]. Transfected cells were expanded in tissue culture and the diL2Kx4-7 and 2C11x4-7 constructs purified from culture supernatant as described earlier [23].

BscCD19xCD3 BiTE was used as an irrelevant control BiTE. Production and purification of bscCD19xCD3 was essentially as described elsewhere [6, 8]. In all experiments, the monomeric form of bispecific antibodies was used.

Effector cell preparation

Human PBMCs

Leukocyte filters were obtained from the 'amtlicher Blutspendedienst' (Munich, Germany). Filters were rinsed with PBS/20% Biocoll and PBMCs isolated by density gradient centrifugation according to standard protocols.

Mouse splenocytes

After removing the spleen, a single-cell suspension was prepared by grinding the organ through a nylon mesh (Reichelt Chemie Technik, Heidelberg, Germany, pore size 51 μm). Erythrocytes were lysed by incubating cells in 4 ml ACK buffer (0.15 M NH_4Cl, 1 mM $KHCO_3$, 0.1 mM Na_2EDTA) for 4 min at room temperature. The reaction was stopped by washing cells with RPMI 1640 10% FCS (Invitrogen, Karlsruhe, Germany).

CD3 T cell enrichment

Murine CD3-positive cells were prepared by using the T cell enrichment column kit from R&D systems (Wiesbaden, Germany) for mouse T cells according to the manufacturer's manual. Briefly, cells were washed twice in PBS (Invitrogen, Karlsruhe, Germany), resuspended in wash-buffer, applied on the T-cell enrichment column and incubated for 10 min at room temperature. CD3-positive cells were eluted by three 2-ml washes with wash-buffer. Purity of enriched CD3-positive splenocytes was determined by flow cytometry.

FACS-based cytotoxicity assay

The fluorescent membrane dye PKH-26 (Sigma, Taufkirchen, Germany) was used to label target cells and to distinguish target from effector cells upon FACS analysis. PKH-26 labeling was performed using the PKH-26 Kit (Sigma, Taufkirchen, Germany). Briefly, 1×10^7 target cells were washed twice in PBS, resuspended in 0.5 ml solution C, mixed with 0.5 ml solution C containing 5 μl PKH-26 and incubated for 2 min at room temperature. After two washes in cell culture medium, target cells were adjusted to a density of 8×10^5 cells/ml and mixed with effector cells (8×10^6 cells /ml) in RPMI 1640 10% FCS at an effector-to-target ratio of 10:1.50 μl of this suspension were seeded per well in 96-well U-bottom microtiter plates (Greiner, Solingen, Germany) and 50 μl of serial BiTE dilutions added. After 20 or 40 h incubation at 37°C/5% CO_2, propidium iodide was added to a final concentration of 1 μg/ml and samples were analyzed in a FACSCalibur flow cytometer (Becton Dickinson, Heidelberg, Germany). CellQuest Pro software from Becton Dickinson was used to collect and analyze the data. Non-viable cells were excluded using forward and side scatter electronic gating. Quantification of cytotoxicity was based on the number of live target cells in the control samples (without antibody) compared to the number of live target cells in the test samples (with serial antibody dilutions). The specific cytotoxicity was calculated by the formula: [1-live target cells (sample)/live target cells (control)]×100. Sigmoidal dose response curves typically had R^2 values > 0.9 as determined by Prism Software (GraphPad Software, San Diego, CA).

Animal studies

In vivo experiments were performed in 6–10-week old immunocompetent C57BL/6 (Charles River, Sulzfeld, Germany) or immunodeficient NOD/SCID mice (Jackson Laboratory, Bar Harbor, USA). NOD/SCID mice were used for the establishment of human xenograft models since they are deficient for T-, B-, NK-cells and show a high tumor take rate when injected with human tumor cell lines. The mice were maintained under sterile and standardized environmental conditions (20 ± 1°C room temperature, 50 ± 10% relative humidity, 12-h light–dark rhythm). Mice received autoclaved food and bedding (ssniff, Soest, Germany) and acidified (pH 4.0) drinking water ad libitum. NOD/SCID mice were tested for leakiness of immunodeficiency and only mice with IgG levels below 100 ng/ml were used. All experiments were performed according to the German Animal Protection Law with permission from the responsible local authorities. In compliance with the Animal Protection Law, mice had to be euthanized when tumor volumes exceeded 10% of their body weight. Statistical analysis of the mean tumor volume of the corresponding treatment groups versus the vehicle control group was performed using the Student's *t* test.

Pharmacokinetic analysis

Fifteen C57BL/6 mice were intravenously injected with 150 μg of either 2C11x4-7 or diL2Kx4-7 per animal and allocated to three different groups of five mice each. Different groups were alternatingly bled at different time points after 2C11x4-7 or diL2Kx4-7 injection (predose, 2, 15, 30 min., and 1, 2, 4, 6, 8, 10 and 24 h) and plasma concentrations quantified by specific ELISAs.

For His-tagged diL2Kx4-7 quantification, ELISA plates (NUNC, Wiesbaden, Germany) were coated with 100 µl (2 µg/ml) of anti-His antibody (Penta-His; Qiagen, Hilden, Germany) and for FLAG-tagged 2C11x4-7, plates were coated with 100 µl (10 µg/ml) of soluble Ep-CAM (Micromet AG, Munich, Germany). Plates were incubated overnight at 4°C and blocked by PBS/1% bovine serum albumin (BSA) for 60 min at 25°C. Test samples were diluted in PBS/10% mouse plasma pool, 100 µl added per well and incubated for 60 min at 25°C. For diL2Kx4-7 quantification, plates were incubated with 100 µl of soluble Ep-CAM protein conjugated with biotin (Micromet, Munich, Germany) at a final concentration of 2 µg/ml for 60 min at 25°C followed by incubation for 60 min at 25°C with 100 µl streptavidin conjugated with alkaline phosphatase (Dako, Hamburg, Germany) at a final concentration of 0.5µg/ml. For 2C11x4-7 quantification, plates were incubated with 100 µl of mouse anti-FLAG conjugated with alkaline phosphatase (Sigma, Taufkirchen, Germany) for 60 min at 25°C. Finally plates were incubated with 100 µl of substrate (1 mg/ml of p-NPP dissolved in 0.2 M TRIS buffer; Sigma) for 20 min at 25°C and the absorbance (405 nm) read on Power WaveX select (Bio-Tek instruments, USA).

The actual 2C11x4-7 and diL2Kx4-7 concentration in the different test samples was calculated referring to a 2C11x4-7 and diL2Kx4-7 standard calibration curve.

Pharmacokinetic calculations of 2C11x4-7 and diL2Kx4-7 were performed by the pharmacokinetic software package WinNonlin Professional 4.1 (Pharsight Corporation, Mountain View, CA; 2003). Parameters were determined by non-compartmental analysis (NCA). The non-compartmental analysis was based on model 201 (intravenous bolus injection). The distribution half-life ($T_{1/2\text{-alpha}}$) was calculated using a log-linear regression of the first four sampling time points, whereas the terminal elimination half-life $t_{1/2\text{-beta}}$ was calculated by the last four sampling time points with a measurable concentration of 2C11x4-7 and diL2Kx4-7 (4 –10 h). For a better estimation of the terminal elimination rate constant, the first value below the lower level of quantification (LLOQ = 1 µg/ml) was set to 1/2 LLOQ (0.5 µg/ml) and also included for the calculations.

SW480 human colon carcinoma xenograft model in NOD/SCID mice

Five $\times 10^6$ human PBMC were mixed with 5×10^6 SW480 colon carcinoma cells in a final volume of 0.2 ml PBS and the effector/target cell mixture (E:T = 1:1) was subcutaneously injected into the right flank of NOD/SCID mice. Six animals per group were intravenously treated with different doses (0.1 and 1 µg/injection) of diL2Kx4-7 or PBS control vehicle starting 1 h after SW480/PBMC inoculation and treatment was repeated for four consecutive days. Tumors were measured on the indicated days with a caliper in two perpendicular dimensions and tumor volumes calculated according to the formula: tumor volume = $[(\text{width}^2 \times \text{length})/2]$.

Syngeneic B16F10/Ep-CAM tumor model in immunocompetent C57BL/6 mice

Two different variants of the B16F10/Ep-CAM tumor model (subcutaneous solid tumor model and lung tumor colony-forming model) have been developed. In the subcutaneous solid tumor model immunocompetent C57B L/6 mice were subcutaneously injected with 7.5×10^4 B16F10/Ep-CAM or B16F10 wildtype cells whereas in the lung tumor, colony-forming model 1×10^5 B16F10/Ep-CAM tumor cells were intravenously injected. In the B16F10/EpCAM tumor models, animals were intravenously treated with different doses of 2C11x4-7 (0.05 – 50 µg/injection), PBS control buffer or an irrelevant BiTE molecule (bscCD19xCD3) specific for human CD3 and human CD19 but not for human Ep-CAM. Both, the early treatment regimens which started 1 h after tumor inoculation as well as the delayed treatment regimens which started at day 5, 7 and 10 after tumor inoculation have been tested. In the subcutaneous model, tumor volumes were measured on the indicated days with a caliper in two perpendicular dimensions and tumor volumes calculated according to the formula: tumor volume = $[(\text{width}^2 \times \text{length})/2]$. In the lung tumor colony-forming model animals were sacrificed at day 21 after intravenous tumor cell inoculation and the number of B16F10/Ep-CAM colonies in lungs determined.

Results

Ep-CAM and CD3 binding properties of diL2Kx4-7 and 2C11x4-7

DiL2Kx4-7 and 2C11x4-7 share in their C-terminal portions the same anti-Ep-CAM single-chain antibody, which was derived from a phage display approach by panning with the extracellular domain of recombinant human Ep-CAM. The N-terminal CD3 binding portions of the bispecific antibodies were different in that they either recognized CD3 on human or murine T cells (Fig.1a). The human CD3-specific BiTE diL2Kx4-7 was generated using a single-chain antibody derived from antibody L2K with specificity for the epsilon subunit of the human CD3 complex [28]. The murine-specific BiTE 2C11x4-7 was generated using a single-chain antibody derived from monoclonal antibody 145-2C11, which has specificity for the epsilon subunit of murine CD3 [24].

The binding properties of diL2Kx4-7 and 2C11x4-7 to Ep-CAM and CD3 were characterized by plasmon resonance analysis using detector chips coated with recombinant human Ep-CAM, and by saturation binding analyses to human and murine T cells, respectively. The equilibrium dissociation constants (K_D) for the Ep-CAM binding arms were not significantly different and

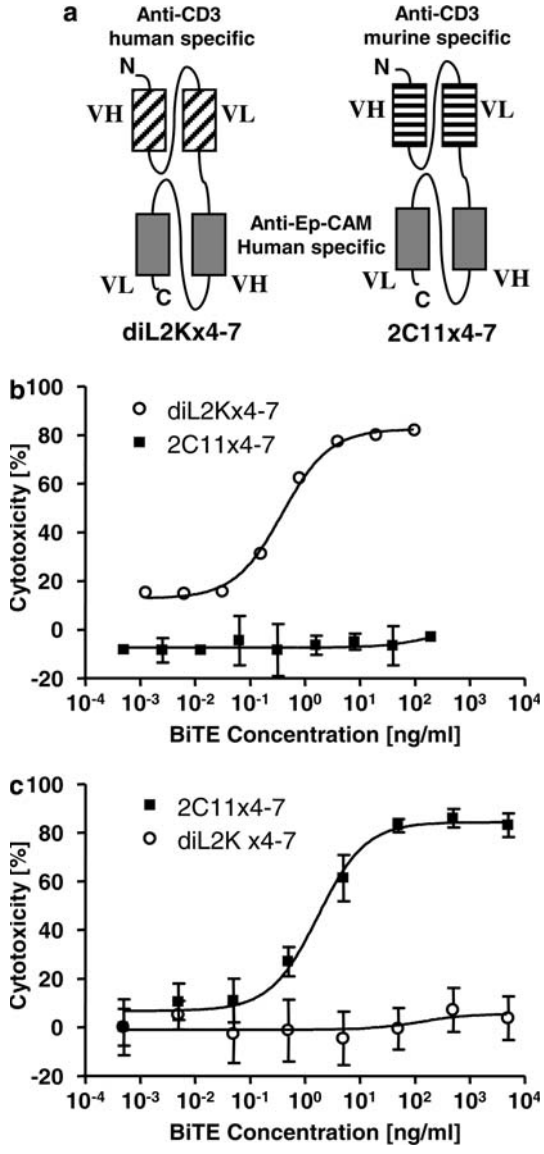

Fig. 1 Structure and in vitro efficacy of BiTEs diL2Kx4-7 and 2C11x4-7 **a** Molecular design of human CD3-specific BiTE diL2Kx4-7 and murine CD3-specific BiTE 2C11x4-7. *Rectangles* depict variable immunoglobulin domains, and *connecting lines* are linker sequences. N, N terminus; C, C terminus. **b** In vitro efficacy of BiTE diL2Kx4-7. Redirected lysis of Kato III tumor cells was tested with human PBMC in the presence of increasing BiTE concentrations for a 20-h assay period. **c** In vitro efficacy of BiTE 2C11x4-7. Redirected lysis of human Ep-CAM cDNA transfected NALM-6 B lymphoma cells was tested with murine CD3 cell-enriched splenocytes in the presence of increasing BiTE concentrations for a 45-h assay period. Effector and target cells were mixed at an E:T ratio of 10:1 *Error bars* indicate SEM of triplicate measurements. Cell lysis was assessed via a FACS based cytotoxicity assay described in Materials and methods

were 52.7 ± 15.4 nM and 58.3 ± 9.6 nM for diL2Kx4-7 and 2C11x4-7, respectively. Saturation binding to human and murine T cells respectively revealed dissociation constants (K_D) for the CD3 binding arms of 19.5 ± 18.1 nM for diL2Kx4-7 and 92 nM for 2C11x4-7, indicating an approximately five fold higher affinity of diL2Kx4-7 for human CD3 than 2C11x4-7 for murine CD3.

Redirected in vitro target cell lysis by diL2Kx4-7 and 2C11x4-7

The bioactivity of diL2Kx4-7 and 2C11x4-7 was assessed by flow cytometry-based in vitro cytotoxicity assays using human PBMCs as effector cells for diL2Kx4-7, and freshly isolated murine CD3-enriched splenocytes as effector cells for 2C11x4-7 at an E–T ratio of 10:1.

DiL2Kx4-7 induced a robust and dose-dependent redirected lysis of Kato III human gastric carcinoma cells in the presence of human T cells, (Fig. 1b). Half maximal cell lysis (EC_{50}) was reached at a concentration of approximately 0.4 ng/ml, i.e., 7 pM. Incubation of Kato III cells with human T cells in the absence of diL2Kx4-7, with diL2Kx4-7 in the absence of T cells (data not shown), or with the murine-specific BiTE 2C11x4-7 in the presence of human T cells did not induce significant redirected lysis of Kato III tumor cells in the presence of human Tcells (Fig. 1b). Redirected lysis induced by 2C11x4-7 showed a reciprocal specificity (Fig. 1c). 2C11x4-7 was very active in redirected lysis of Ep-CAM cDNA-transfected NALM-6 lymphoma cells with murine T cells, while human CD3-specific BiTE diL2Kx4-7 was completely inactive with murine T cells against transfected NALM-6 cells. To achieve a >80% target cell lysis, 2C11x4-7 required 45 h using murine T cells, while diL2Kx4-7 required 20 h using human T cells. Half maximal target cell lysis (EC_{50}) of 2C11x4-7 was seen at a concentration of approximately 1.9 ng/ml (34 pM); i.e., five times higher than that of diL2Kx4-7.

Pharmacokinetic properties of diL2Kx4-7 and 2C11x4-7

C57BL/6 mice were intravenously injected with 150 μg 2C11x4-7 or diL2Kx4-7, respectively, and mice bled at different time points. 2C11x4-7 and diL2Kx4-7 plasma concentrations were quantified by specific ELISAs and plasma concentration versus time profiles generated (Fig. 2a).

Peak plasma concentrations of 2C11x4-7 and diL2Kx4-7 in C57BL/6 mice were detected 2 min after bolus i.v. injection and reached the lower limit of quantification of 1 μg/ml within approximately 8–10 h. Plasma concentration versus time curves of 2C11x4-7 and diL2Kx4-7 exhibited a bi-exponential curve progression with an early distribution phase between 0 and 1 h and a terminal elimination phase. Elimination rate constants were determined and resulted in distribution half-lives ($T_{1/2\text{-alpha}}$) of 0.44 ± 0.03 and 0.35 ± 0.01 h and terminal elimination half-lives ($T_{1/2\text{-beta}}$) of 2.7 ± 0.12 and 3.6 ± 0.15 h for 2C11x4-7 and diL2Kx4-7, respectively (Fig. 2b). Therefore, short distribution half-lives appeared to be responsible for the rapid decrease in plasma concentrations. Bolus injections of 150 μg of 2C11x4-7

and diL2Kx4-7 resulted in comparable mean pharmacokinetic parameters (Fig. 2b). Based on the in vitro efficacy data and the pharmacokinetic analysis of 2C11x4-7 and diL2Kx4-7, a daily intravenous dosing scheme was selected for the following in vivo efficacy studies.

Antitumor activity of diL2Kx4-7 in human SW480 colon carcinoma xenograft model

In order to evaluate the in vivo efficacy of diL2Kx4-7, the human colon cancer cell line SW480 was used to establish a xenograft model in NOD/SCID mice. A mixture of 5×10^6 unstimulated human PBMC and 5×10^6 Ep-CAM positive SW480 tumor cells (with ca. 540,000 Ep-CAM sites/cell) was subcutaneously injected into the right flank of each mouse, and six animals per group were intravenously treated with either the vehicle PBS, 0.1 or 1 µg diL2Kx4-7 per injection. Treatment was started 1 h after subcutaneous inoculation of PBMC/SW480 cell mixture and repeated once daily for 4 consecutive days. The outgrowth of solid subcutaneous SW480 tumors was determined by caliper measurements and used as an efficacy measure (Fig. 3).

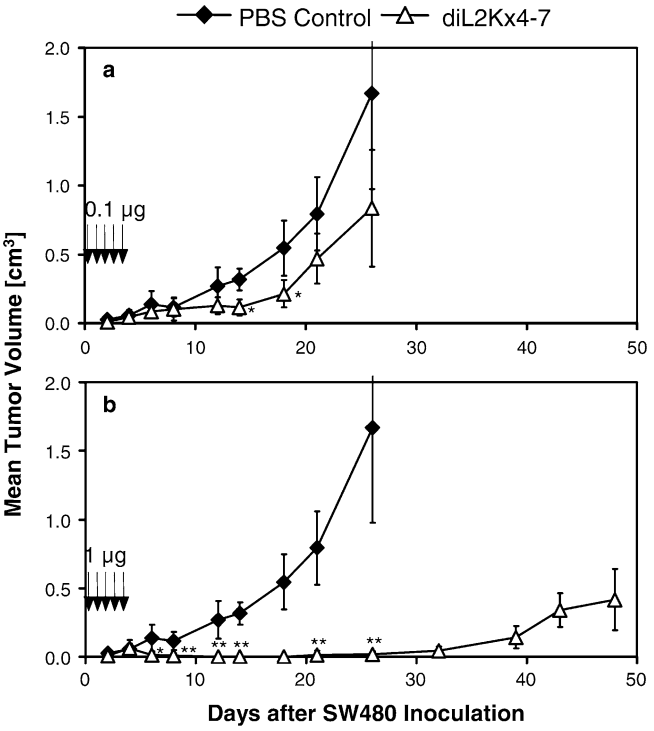

Fig. 3 Dose-dependent inhibition of subcutaneous SW480 tumor growth in NOD/SCID mice by diL2Kx4-7. Five $\times10^6$ SW480 cells were mixed with 5×10^6 human PBMCs (PBMC:T ratio of 1:1) and subcutaneously injected into the right flanks of six female NOD/SCID mice per group. Treatment with 0.1 µg/mouse **a** and 1 µg/mouse **b** of diL2Kx4-7 (*open triangles*) and PBS control buffer (*black diamonds*) was started 1 h after the injection of tumor cells and treatment was repeated for four consecutive days. Tumor size was measured three times a week with calipers. *Arrows* indicate time points of diL2Kx4-7 administration. *Asterisks* indicate statistical differences between the treatment and the control group (*$P \le 0.05$; **$P \le 0.01$ as determined with the Student's *t* test)

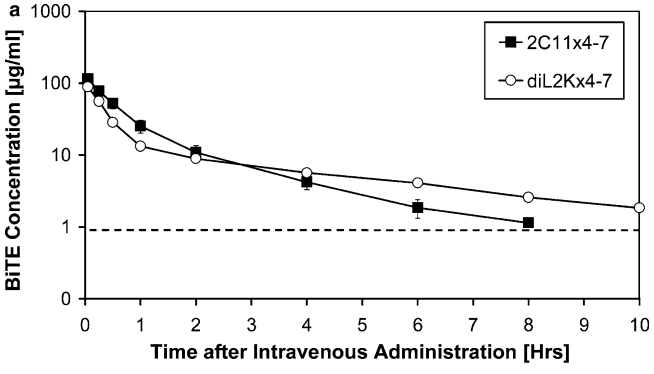

b

2C11x4-7	Dose [µg/mouse]	C_{max} [µg/mL]	$T_{1/2\text{-alpha}}$ [hr]	$T_{1/2\text{-beta}}$ [hr]	AUClast [hr*µg/mL]	Vz [mL]	CL [mL/hr]
Profile 1	150	111.01	0.46	2.59	108.57	5.07	1.36
Profile 2	150	118.72	0.40	2.67	105.48	5.38	1.40
Profile 3	150	123.68	0.43	2.67	111.83	5.08	1.32
Profile 4	150	116.93	0.47	2.90	101.20	6.08	1.45
Profile 5	150	104.75	0.45	2.66	104.86	5.40	1.40
Mean	**-**	**115.02**	**0.44**	**2.70**	**106.39**	**5.40**	**1.39**
SD	**-**	**7.31**	**0.03**	**0.12**	**4.01**	**0.41**	**0.05**

diL2Kx4-7	Dose [µg/mouse]	C_{max} [µg/mL]	$T_{1/2\text{-alpha}}$ [hr]	$T_{1/2\text{-beta}}$ [hr]	AUClast [hr*µg/mL]	Vz [mL]	CL [mL/hr]
Profile 1	150	82.54	0.35	3.50	100.36	7.43	1.47
Profile 2	150	92.12	0.35	3.78	104.86	7.67	1.41
Profile 3	150	94.87	0.34	3.44	103.50	7.08	1.43
Profile 4	150	91.72	0.34	3.76	98.06	8.16	1.50
Profile 5	150	80.04	0.36	3.65	100.69	7.73	1.47
Mean	**-**	**88.26**	**0.35**	**3.63**	**101.49**	**7.61**	**1.46**
SD	**-**	**6.54**	**0.01**	**0.15**	**2.70**	**0.40**	**0.04**

Fig. 2 Pharmacokinetic parameters of 2C11x4-7 and diL2Kx4-7 C57BL/6 mice were intravenously injected with 150 µg 2C11x4-7 or diL2Kx4-7 and groups of five mice each bled at different time points. Plasma concentrations of BiTEs were quantified by specific ELISAs. **a** Plasma concentration versus time profiles of 2C11x4-7 and diL2Kx4-7 in C57BL/6 mice. **b** Mean pharmacokinetic parameters of 2C11x4-7 and diL2Kx4-7. The *dashed line* indicates the lower limit of quantification of 1 µg/ml

A dose-dependent antitumor activity of diL2Kx4-7 was observed. Five daily doses of 0.1 µg per injection (Fig 3a) induced a significant reduction of SW480 tumor growth ($P < 0.05$ on day 12, $P < 0.01$ on days 14 and 18). Five daily injections of 1µg diL2Kx4-7 (Fig. 3b) induced a more pronounced anti-tumor effect. After an initial outgrowth of very small tumors on day 4 with a mean tumor size of 0.064 cm^3, complete suppression of tumor outgrowth was seen until day 32 after SW480 inoculation, indicating an approximately 30-day delay in disease onset in comparison with the control vehicle. From day 12 to the end of the study, tumor size was significantly smaller as compared to vehicle-treated animals ($P < 0.01$) and to the low dose of 0.1 µg diL2Kx4-7.

Establishment of efficacy models in immunocompetent mice using the murine CD3-specific BiTE 2C11x4-7

In order to test the in vivo efficacy of the murine CD3-specific BiTE 2C11x4-7 in immunocompetent animals, we used C57BL/6 mice and a syngeneic tumor model. The murine melanoma cell line B16F10/Ep-CAM

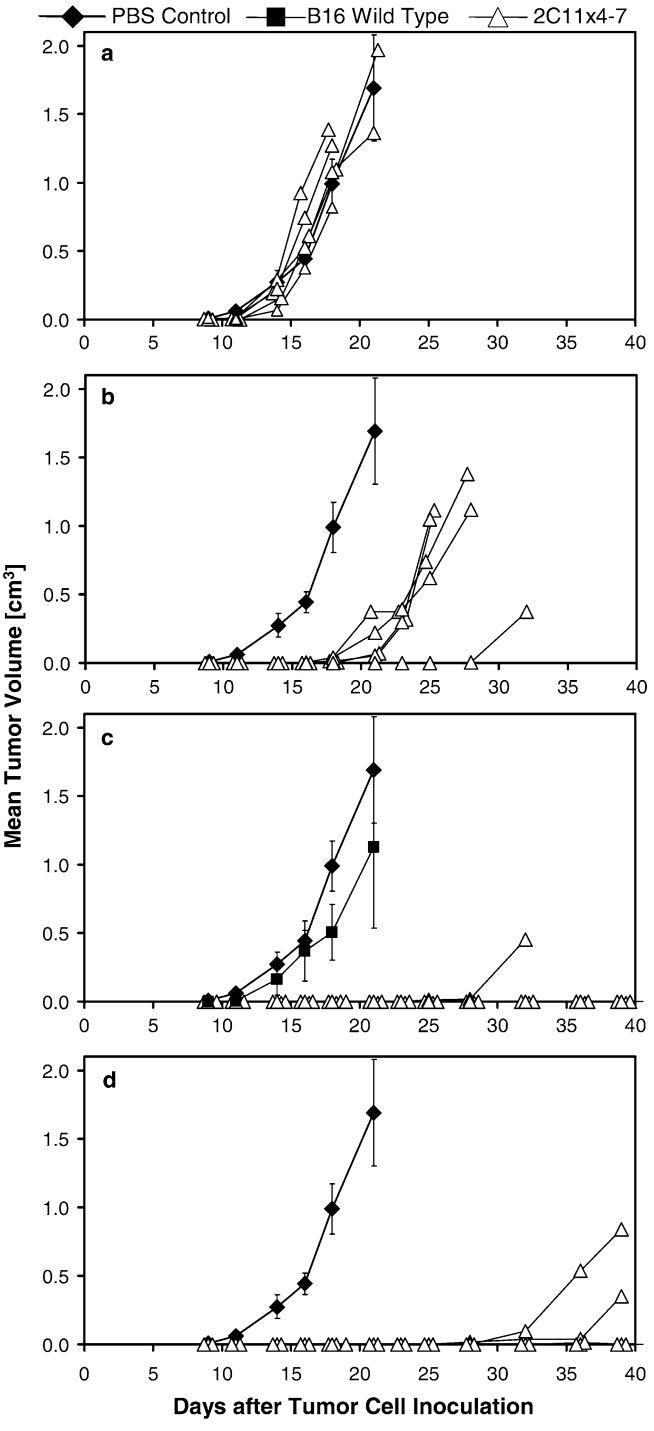

Fig. 4 Effect of the 2C11x4-7 dose on subcutaneous B16F10/Ep-CAM tumor growth in immunocompetent C57BL/6 mice. B16F10/Ep-CAM or B16F10 wildtype (B16F10WT) tumor cells (7.5×10^4) were subcutaneously injected into the right flanks of 5 C57BL/6 mice per group and tumor size measured three times a week. Treatment with PBS control buffer and different doses of 2C11x4-7 (**a** 0.05), (**b** 0.5), (**c** 5) and (**d** 50 μg/injection) was started 1 h after the injection of tumor cells and treatment was repeated for four consecutive days. One group of control animals (*black diamonds*) was implanted with B16F10/Ep-CAM and treated with PBS control buffer, whereas another group of control animals (*black squares*; **c**) was implanted with B16F10WT target-negative tumor cells and treated with 5 μg 2C11x4-7/injection. For the control groups, mean values of tumor volume are shown, whereas for the 2C11x4-7 treatment groups, individual tumor growth curves are depicted (*open triangles*). *Error bars* indicate standard deviation calculated for the mean value of tumor growth curves. *Arrows* indicate time points of 2C11x4-7 administration

expressing human Ep-CAM (57,000 Ep-CAM binding sites/cell) was used to establish both a local subcutaneous tumor and a disseminated lung tumor colony-forming model. In the local tumor model, subcutaneous injection of 7.5×10^4 B16F10/Ep-CAM melanoma cells resulted in a 100% tumor take with first palpable tumors detectable 12 days after inoculation. In the lung tumor colony-forming model, intravenous injection of 1×10^5 B16F10/Ep-CAM melanoma cells resulted in an average of 50 lung tumor colonies at day 21 after inoculation. In both efficacy models, early 2C11x4-7 treatment starting 1 h after tumor cell inoculation was performed to simulate an early disease setting, whereas late BiTE treatment on days 5, 7 and 10 was used as a more advanced disease setting.

Anti-tumor activity of 2C11x4-7 after early treatment

With respect to the kinetics of tumor growth, the syngeneic s.c. tumor model shown in Fig. 4 came closest to the human xenograft SW480 model (Fig. 3). Five animals per group were subcutaneously injected with 7.5×10^4 B16F10/Ep-CAM tumor cells and intravenously injected with PBS control vehicle or the indicated doses of 2C11x4-7. One group of animals was injected with B16F10 wildtype tumor cells (B16F10WT) not expressing human Ep-CAM and treated with 5 μg/injection 2C11x4-7 to evaluate the target specificity of 2C11x4-7 treatment (Fig. 4c).

Treatment with 2C11x4-7 induced a dose-dependent growth inhibition of human Ep-CAM expressing B16F10/Ep-CAM tumors. The lowest dose level of 0.05 μg/injection had no significant effect on B16F10/Ep-CAM tumor growth (Fig. 4a). Doses of 0.5 μg/injection induced a significant reduction ($P < 0.025$) in B16F10/Ep-CAM tumor growth, but with a delay of approximately 10 days, all animals developed tumors (Fig. 4b). With 5 or 50 μg BiTE per injection, tumor outgrowth was completely inhibited in all mice until day 28 (Fig. 1c, d). At the end of the study on day 39, three out of five and four out of five animals were still free of tumor in the 5- and 50-μg dose groups, respectively. The outgrowth of Ep-CAM-negative B16F10WT tumors could not be prevented by 5 μg doses of 2C11x4-7 (Fig. 4c), showing the dependence of anti-tumor effects on the target antigen Ep-CAM. In both control groups, five out of five mice developed large subcutaneously growing tumors.

In vivo efficacy of 2C11x4-7 upon delayed treatment

A dose of 5 μg per injection (see Fig. 4) was selected for testing the antitumor activity of delayed treatments with 2C11x4-7. Treatments started on day 0 or were delayed until days 5, 7 and 10 after tumor inoculation, and performed for 9 consecutive days. Eight animals were either treated on days 5–14 with PBS control vehicle or 5 μg/injection of a control BiTE specific for human CD3 and human CD19 [6, 8] (Fig. 5).

Early treatment with 2C11x4-7 on days 0 – 9 induced complete inhibition of tumor growth until day 22 after tumor cell inoculation (Fig. 5a). At day 26, five out of eight animals were still free of tumor. Delayed treatment from days 5 –14 induced complete inhibition of tumor growth until day 19, and at day 26 two out of eight animals were still free of tumor (Fig. 5b). Delayed treatment from days 7 – 16 induced complete inhibition of tumor growth until day 15, but thereafter all animals developed tumors (Fig. 5c). Finally, treatment from days 10 – 19 no longer induced complete inhibition of tumor growth but tumor growth was still well controlled and significantly different ($P < 0.0005$) compared to the PBS and control BiTE groups that were treated from days 5–14.

Activity of 2C11x4-7 in a lung tumor colony-forming model

To evaluate the efficacy of 2C11x4-7 in a disseminated tumor setting, we performed an early and late treatment experiment in a lung tumor colony-forming model using B16F10/Ep-CAM cells. Eight animals per group were intravenously injected with 1×10^5 B16F10/Ep-CAM melanoma cells and intravenously treated with PBS control vehicle or 5 μg 2C11x4-7 per injection daily for 10 consecutive days. In the early treatment group, treatment with BiTE 2C11x4-7 was started 1 h after tumor inoculation and in the delayed treatment group 5 days later. Three weeks after B16F10/Ep-CAM tumor cell inoculation, animals were sacrificed and the number of lung tumor colonies quantified as a measure for efficacy (Fig. 6a, 6b).

PBS treatment from days 0 – 9 resulted on average, in 50 macroscopically detectable tumor colonies per lung. Early treatment with 2C11x4-7 from days 0 – 9 almost completely prevented the formation of B16F10/Ep-CAM lung tumor colonies. Seven out of eight animals had lungs free of tumors; in one animal only a single small colony was found (Fig. 6a, 6b; $P \ll 0.0001$ as compared to the PBS control group). Delayed treatment with 2C11x4-7 from days 5–14 was also highly efficacious in preventing lung tumor colony formation. Lungs in three out of eight animals were completely free of tumor at the end of the study and in the tumor-positive animals, the number of detectable lung tumor colonies

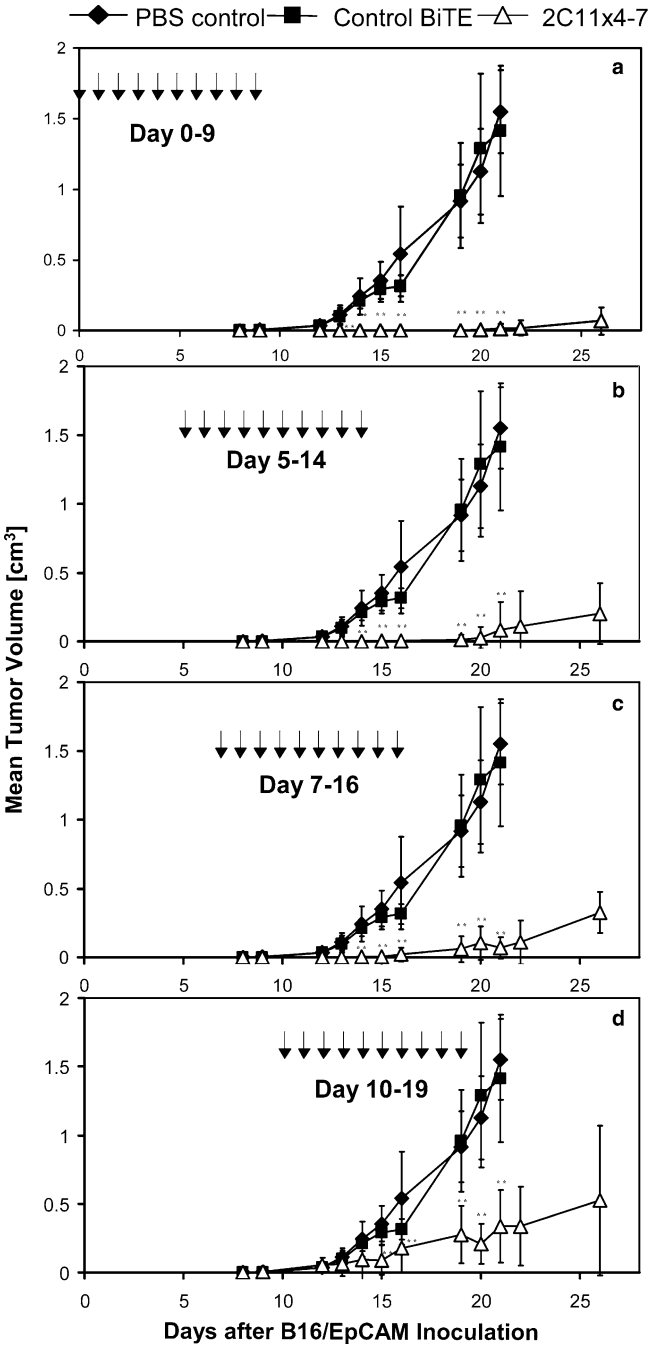

Fig. 5 Effect of delayed 2C11x4-7 treatments on the growth of established subcutaneous B16F10/Ep-CAM tumors in immunocompetent mice. B16F10/Ep-CAM cells (7.5×10^4) were subcutaneously injected into the right flanks of eight immunocompetent C57BL/6 mice per group and tumor size measured three times a week. Treatment with 5 μg 2C11x4-7/mouse (*open triangles*) was started at different time points (day 0, 5, 7 and 10) after the injection of tumor cells and treatment was repeated for nine consecutive days. One group of control animals (*black diamonds*) was treated with PBS control buffer whereas another group of control animals (*black squares*) was treated with 5 μg/injection of an irrelevant BiTE molecule from days 5–14. *Small double asterisks* indicate highly significant differences ($P < 0.0005$) compared to the PBS control group

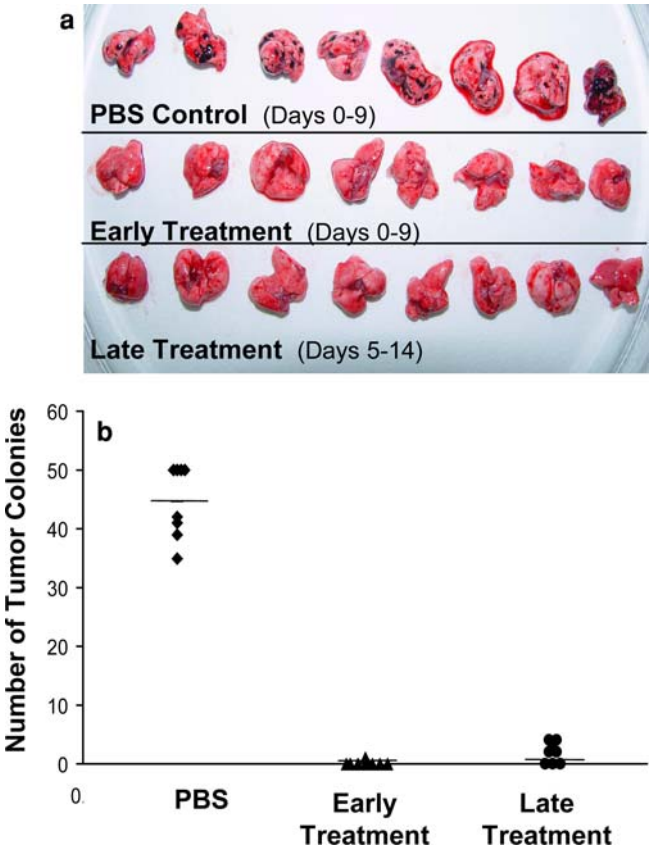

Fig. 6 Effects of early and late treatment with BiTE 2C11x4-7 on the development of B16F10/Ep-CAM lung tumor colonies in C57BL/6 mice. B16F10/Ep-CAM cells (1×10^5) were intravenously injected into the tail vein of eight immunocompetent C57BL/6 mice per group. Animals were treated with 5 μg/mouse 2C11x4-7 on day 0 (early treatment) or day 5 (late treatment), or PBS control buffer 1 h after intravenous B16F10/Ep-CAM inoculation, and treatment was repeated for nine consecutive days. 2C11x4-7 treatment groups were split into an early (day 0–9) and late treatment group (day 5–14). Twenty-one days after tumor cell inoculation animals were sacrificed, lungs removed, and the number of lung tumor colonies quantified as a measure of efficacy. **a** Photographs of lungs of animals from day 21. **b** Number of lung tumor colonies as individual readings (*symbols*) and the mean numbers (*short lines*) are given for each treatment group ($P = 7\times10^{-12}$ and 2×10^{-11} for early and late treatment, respectively, as determined by the Student's *t* test).

was very low (2–4 per lung) and different from the PBS control group with very high significance ($P \ll 0.0001$). We did not observe any side effects in mice treated with BiTEs.

Discussion

In the present study, we have for the first time tested in parallel BiTEs with specificity for either human or murine CD3 that both recognize the target antigen Ep-CAM by the same single-chain antibody. While the two BiTEs had essentially the same affinity for Ep-CAM, their respective affinities for CD3 were different. Human CD3 was recognized with higher affinity by the human CD3-specific BiTE than murine CD3 was recognized by the murine CD3-specific BiTE. Apart from the approximately five fold difference in CD3 binding affinity, the comparison of the two BiTEs also suffered from the fact that Ep-CAM expression on SW480 target cells was approximately ten fold higher than on transfected B16F10/Ep-CAM melanoma cells. In vivo, the two BiTE constructs could only be compared by using, in one case, an immunodeficient NOD/SCID mouse model supplemented with unstimulated human T cells and, in the other case, an immunocompetent mouse model. In both in vitro and in vivo experiments, the human CD3-specific BiTE, diL2Kx4-7, was somewhat more potent in its biological activity as compared to the murine CD3-specific BiTE. The higher efficacy of the human-specific BiTE could come from the higher affinity for CD3 and the higher Ep-CAM expression on SW480 target cells but it is also possible that human T cells generally respond stronger to stimulation than murine T cells or have higher cytolytic potential. Considerable variation with respect to BiTE efficacy was seen among human donors [6], that exceeded by far the efficacy difference seen here between murine and human CD3-specific BiTEs. It therefore cannot be excluded that variations of donor T cell activity significantly contributed to the observed differences.

Despite differences, the biological activities of human and murine CD3-specific BiTEs were remarkably similar and within the same order of magnitude. The comparable antitumor activities of diL2Kx4-7 in the SW480 model and of 2C11x4-7 in the immunocompetent model (compare Fig. 3 and 4) suggest that T cell abundance and route of T cell administration were not the key determinants for in vivo BiTE efficacy. In the SW40 model, a small number of human T cells was pre-mixed with tumor cells at an effective $CD8^+$ T cell to a target ratio of 1 to 7 (PBMC to target ratio = 1:1). In the immunocompetent model, T cells were present in abundance but had to first penetrate the subcutaneous tumor cell inoculate. Once activated inside the tumor, T cells may, however, rely on a large supply of additional T cells recruitable from the periphery in response to chemokine gradients. Moreover, because of species incompatibilities, human cytokines released by BiTE-activated human T cells in NOD/SCID mice may have less or no systemic effects in mice compared to murine cytokines released by BiTE-activated murine T cells. This may have implications for side-effect profiles of BiTEs but also for efficacy assuming that T cell cytokines and chemokines will lead to attraction, recruitment and activation of other immune cells in tumors. The comparable antitumor activity of the two BiTEs in the two distinct systems suggests that daily BiTE treatments for 5 – 10 days may have compensated for most initial differences with respect to T cell presence, number and supply in tumors, and effects by locally produced cytokines and chemokines.

The two new BiTEs described in this study share all properties described for a CD19xCD3-bispecific BiTE

that was previously analyzed in great detail [6, 7]. With 2C11x4-7 and diL2Kx4-7, we observed again that unstimulated human and, for the first time, murine T cells can be efficiently redirected towards target cell lysis. The independence of T cell costimuli, such as lectins, IL-2 or anti-CD28 antibodies, may come from an optimal juxtaposition of T and target cells by the particular geometry and format of bispecific single-chain antibodies. We have recently analyzed the cytolytic synapses induced by BiTEs in comparison with synapses induced by peptide/MHC class I complexes [12]. This study showed that BiTE-induced lytic synapses are structurally indistinguishable from naturally induced synapses, which may provide one explanation for the high potency of such antibody constructs. Another shared property is the high level of specificity. As shown here, the two BiTEs were specific for their respective CD3 complexes and, despite the same Ep-CAM binding activity, could not induce redirected lysis with T cells from the respective unmatched species (Fig. 1b, c). Likewise binding of murine or human-specific BiTEs to murine or human T cells in the absence of the specific antigen on target cells also did not induce redirected lysis, consistent with data from other BiTEs [6]. Here, we have seen for the first time in animals that a BiTE solely binding to murine T cells does not affect the growth of tumors that lack the target antigen (see Fig. 4c). Lastly, the two BiTEs characterized in this study showed high potency with concentrations for half-maximal in vitro target cell lysis slightly above or below 1 ng/ml, i.e., 18 pM. The high efficacy of the two BiTEs in animals, upon daily i.v. injections for 5 to 10 days, has to be particularly seen in the context of their short half-lives in mice of only 20–25 min and 2–3 h for the distribution and terminal elimination phase.

The obvious loss of efficacy with delayed treatment by 2C11x4-7 in the immunocompetent mouse model is not well understood. B16 tumors grow rather aggressively and are difficult to control once in an exponential growth phase. It is possible that tumors had already reached a size in mice after 10 days that substantially reduced penetrance of the tumor by BiTE and/or T cells. Tumor penetrance by BiTEs does not appear to be an issue. In the SW480 model, we have seen other i.v. administered BiTEs eradicating subcutaneous tumors with sizes of up to 200 mm^3 [13]. The penetrance of peripheral T cells into solid subcutaneous tumors may rather be a limitation of the new model. The B16 tumor cell inoculates may have developed tight cell/cell interaction and intercellular matrix deposits, which could pose a barrier to incoming T cells. The presence of T cells may be less of a problem in natural human tumors, which are very frequently found to contain $CD8^+$ and $CD4^+$ T cells collectively referred to as tumor-infiltrating lymphocytes [29].

How useful is a murine CD3-specific BiTE that can be tested in an immunocompetent mouse model for development of human-specific BiTEs? The use of the entire T cell compartment of an organism rather than a low number of co-administered T cells from a different species is certainly an advantage that brings an immunocompetent model closer to the therapeutically relevant situation. With the use of the syngeneic B16 melanoma line, the target cell line became more physiological than human cancer cell lines in the background of immunodeficient mice, despite the fact that human Ep-CAM expression on the syngeneic transfected tumor cell line was, in fact, much lower as typically found on human epithelial-derived carcinomas [30].

Other groups have previously used syngeneic mouse models to study the therapeutic efficacy of bispecific antibodies [31, 32, 33–35]. Demanet et al. [32] and Brissinck et al. [31] reported cure of murine B-cell lymphomas by treatment with quadroma-derived bispecific antibodies of anti-idiotype and anti-CD3 specificity. Such results could not be obtained with solid tumor models. These and other studies made it clear that therapeutic success with antitumor × anti-CD3 bispecific antibodies is more readily achieved in lymphoma bearing mice than in those challenged with cells forming solid tumors. This can be partially attributed to the fact that lymphoid tumors are more easily accessible to immune effector cells, while subcutaneously growing solid tumors demand an additional migration and penetration step.

Bakacs et al. [35] could induce marked inhibition of solid pulmonary metastases by a bispecific Fab2 without additional co-stimulatory reagents. However, the effect on the survival time of the treated animals was marginal. The higher efficacy of our molecule might be due to the different format. BiTE molecules are smaller than Fab2 fragments which may transform after better penetration into solid subcutaneous tumors. Grosse-Hovest and colleagues [36] have seen positive results by treating C57BL/6 mice intraperitoneally inoculated with B16 melanoma cells with an antitumor × anti-CD3 Fab2 fragment. This therapeutic effect was almost completely lost when treatment was delayed by only one day. In our study, a highly significant inhibition of tumor growth was induced even after delayed treatment regimens with the 2C11x4-7 BiTE. The therapeutic effect of the Fab2 fragment could be improved by co-treating mice with an antitumor × anti-CD28 bispecific antibody. In contrast, BiTEs are capable of efficiently redirecting T-cell cytotoxicity against various different target cells without any requirement for pre- or co-stimulation of effector cells [6, 7].

Perhaps the most impressive antitumor activity was described for a trifunctional bispecific antibody that recognizes T cells by CD3, tumor cells by human Ep-CAM, and accessory immune cells via the Fcγ part [37]. This molecule showed activity in two immunocompetent mouse models and was able to induce protective immunity. We do not know whether BiTEs can induce protective immunity but they appear to be equally potent as trifunctional antibodies although they completely lack binding to antigen-presenting cells (APC). The ab-

sence of Fcγ binding by BiTEs may reduce their immunogenicity and thereby the incidence of neutralizing antibodies to the drug construct. Another issue of trispecific antibodies could be the side effects related to T cell/APC interaction. This interaction can take place in the absence of Ep-CAM-positive tumor cells and may lead to overt systemic cytokine production.

A general limitation of human xenograft models in immunodeficient mice is the predictability of safety issues. In such models side effects of BiTE therapies may only come from tumor cell lysis. The use of murine CD3-specific BiTEs in immunocompetent mice will in addition reveal side effects coming from polyclonal T cell activation, such as cytokine release syndromes. However, no such side effects were observed in the present study even at high doses of 50 μg per injection. In conclusion, the present models provide a next important step in the preclinical development of new BiTE therapies. They allow for the selection of appropriate BiTE targets to optimize and study BiTE formulations and routes of administration, to study BiTE pharmacokinetics and tissue distribution, and to predict side effects related to tumor lysis and polyclonal T cell activation.

References

1. Perez P, Hoffman RW, Shaw S, Bluestone JA, Segal DM (1985) Specific targeting of cytotoxic T cells by anti-T3 linked to anti-target cell antibody. Nature 316:354–356
2. Staerz UD, Kanagawa O, Bevan MJ (1985) Hybrid antibodies can target sites for attack by T cells. Nature 314:628–631
3. Kufer P, Lutterbuse R, Baeuerle PA (2004) A Revival of bispecific antibodies. Trends Biotechnol 22:238–244
4. Talac R, Nelson H (2000) Current perspectives of bispecific antibody-based immunotherapy. J Biol Regul Homeost Agents 14:175–181
5. Baeuerle PA, Kufer P, Lutterbuse R (2003) Bispecific antibodies for polyclonal T-cell engagement. Curr Opin Mol Ther 5:413–419
6. Dreier T, Lorenczewski G, Brandl C, Hoffmann P, Syring U, Hanakam F, Kufer P, Riethmuller G, Bargou R, Baeuerle PA (2002) Extremely potent rapid and costimulation-independent cytotoxic T-cell response against lymphoma cells catalyzed by a single-chain bispecific antibody. Int J Cancer 100:690–697
7. Dreier T, Baeuerle PA, Fichtner I, Grun M, Schlereth B, Lorenczewski G, Kufer P, Lutterbuse R, Riethmuller G, Gjorstrup P, Bargou RC (2003) T cell costimulus-independent and very efficacious inhibition of tumor growth in mice bearing subcutaneous or leukemic human B cell lymphoma xenografts by a CD19-/CD3- bispecific single-chain antibody construct. J Immunol 170:4397–4402
8. Loffler A, Kufer P, Lutterbuse R, Zettl F, Daniel PT, Schwenkenbecher JM, Riethmuller G, Dorken B, Bargou RCA (2000) recombinant bispecific single-chain antibody, CD19 x CD3, induces rapid and high lymphoma-directed cytotoxicity by unstimulated T lymphocytes. Blood 95:2098–2103
9. Loffler A, Gruen M, Wuchter C, Schriever F, Kufer P, Dreier T, Hanakam F, Baeuerle PA, Bommert K, Karawajew L, Dorken B, Bargou RC (2003) Efficient elimination of chronic lymphocytic leukaemia B cells by autologous T cells with a bispecific anti-CD19/anti-CD3 single-chain antibody construct. Leukemia 17:900–909
10. Zocher M, Baeuerle PA (2004) Bispecific single-chain antibody fusion protein for targeted depletion of autoreactive B cells via unstimulated human T lymphocytes. Mol Immunol 41:511–518
11. Hoffmann P, Hofmeister R, Brischwein K, Brandl C, Crommer S, Bargou R, Itin C, Prang N, Baeuerle PA (2005) Serial killing of tumor cells by cytotoxic T cells redirected with a CD19-/CD3-bispecific single-chain antibody construct. Int J Cancer
12. Offner S, Romaniuk A, Kufer P, Baeuerle PA (2005) Induction of Regular Cytolytic T Cell Synapses by Bispecific Single-Chain Antibody Constructs on MHC Class I-negative Tumor Cells. Mol Immunol
13. Schlereth B, I Fichtner I, Lorenczewski G, Kleindienst P, Brischwein K, da Silva A, Kufer P, Lutterbuese R, Junghahn I, Kasimir-Bauer S, Wimberger P, Kimmig R, Baeuerle PA (2005) Eradication of Tumors from a Human Colon Cancer Cell Line and from Ovarian Cancer Metastases in Immunodeficient Mice by a Single-chain Ep-CAM-/CD3-bispecific Antibody Construct. Cancer Res
14. Went PT, Lugli A, Meier S, Bundi M, Mirlacher M, Sauter G, Dirnhofer S (2004) Frequent EpCam protein expression in human carcinomas. Hum Pathol 35:122–128
15. Litvinov SV, Velders MP, Bakker HA, Fleuren GJ, Warnaar SO (1994) Ep-CAM: a human epithelial antigen is a homophilic cell-cell adhesion molecule. J Cell Biol 125:437–446
16. Schmitt M, Schmitt A, Reinhardt P, Thess B, Manfras B, Lindhofer H, Riechelmann H, Wiesneth M, Gronau S (2004) Opsonization with a trifunctional bispecific (alphaCD3 x alphaEpCAM) antibody results in efficient lysis in vitro and in-vivo of EpCAM positive tumor cells by cytotoxic T lymphocytes. Int J Oncol 25:841–848
17. Di Paolo C, Willuda J, Kubetzko S, Lauffer I, Tschudi D, Waibel R, Pluckthun A, Stahel RA, Zangemeister-Wittke U (2003) A recombinant immunotoxin derived from a humanized epithelial cell adhesion molecule-specific single-chain antibody fragment has potent and selective antitumor activity. Clin Cancer Res 9:2837–2848
18. Adkins JC, Spencer CM (1998) Edrecolomab (monoclonal antibody 17–1A). Drugs 56:619–626; discussion 627–618
19. de Bono JS, Tolcher AW, Forero A, Vanhove GF, Takimoto C, Bauer RJ, Hammond LA, Patnaik A, White ML, Shen S, Khazaeli MB, Rowinsky EK, LoBuglio AF (2004) ING-1, a monoclonal antibody targeting Ep-CAM in patients with advanced adenocarcinomas. Clin Cancer Res 10:7555–7565
20. Naundorf S, Preithner S, Mayer P, Lippold S, Wolf A, Hanakam F, Fichtner I, Kufer P, Raum T, Riethmuller G, Baeuerle PA, Dreier T (2002) In vitro and in vivo activity of MT201, a fully human monoclonal antibody for pancarcinoma treatment. Int J Cancer 100:101–110
21. Poncelet P, Carayon P (1985) Cytofluorometric quantification of cell-surface antigens by indirect immunofluorescence using monoclonal antibodies. J Immunol Methods 85:65–74
22. Porwit-MacDonald A, Janossy G, Ivory K, Swirsky D, Peters R, Wheatley K, Walker H, Turker A, Goldstone AH, Burnett A (1996) Leukemia-associated changes identified by quantitative flow cytometry IV CD34 overexpression in acute myelogenous leukemia M2 with t(8;21). Blood 87:1162–1169
23. Kufer P, Zettl F, Borschert K, Lutterbuse R, Kischel R, Riethmuller G (2001) Minimal costimulatory requirements for T cell priming and TH1 differentiation: activation of naive human T lymphocytes by tumor cells armed with bifunctional antibody constructs. Cancer Immun 1:10
24. Leo O, Foo M, Sachs DH, Samelson LE, Bluestone JA (1987) Identification of a monoclonal antibody specific for a murine T3 polypeptide. Proc Natl Acad Sci USA 84:1374–1378
25. Mack M, Riethmuller G, Kufer PA (1995) small bispecific antibody construct expressed as a functional single-chain molecule with high tumor cell cytotoxicity. Proc Natl Acad Sci USA 92:7021–7025

26. Sambrook J, Russel DW (2001) Molecular Cloning, a laboratory manual, 3rd edn. Cold Spring Habor Laboratory Press, New York
27. Kaufman RJ (1990) Selection and coamplification of heterologous genes in mammalian cells. Methods Enzymol 185:537–566
28. Brischwein K, Schlereth B, Guller B, Steiger C, Wolf A, Lutterbuese R, Offner S, Locher M, Urbig T, Raum T, Kleindienst P, Wimberger P, Kimmig R, Fichtner I, Kufer P, da Silva A, Baeuerle PA (2005) MT110: A Novel Bispecific Single-chain Antibody Construct with High Efficacy in Eradicating Established Tumors. Mol Immunol
29. Balch CM, Riley LB, Bae YJ, Salmeron MA, Platsoucas CD, von Eschenbach A, Itoh K (1990) Patterns of human tumor-infiltrating lymphocytes in 120 human cancers. Arch Surg 125:200–205
30. Prang N, Preithner S, Brischwein K, Goster P, Woppel A, Muller J, Steiger C, Peters M, Baeuerle PA, da Silva AJ (2005) Cellular and complement-dependent cytotoxicity of Ep-CAM-specific monoclonal antibody MT201 against breast cancer cell lines. Br J Cancer 92:342–349
31. Brissinck J, Demanet C, Moser M, Leo O, Thielemans K (1991) Treatment of mice bearing BCL1 lymphoma with bispecific antibodies. J Immunol 147:4019–4026
32. Demanet C, Brissinck J, Van Mechelen M, Leo O, Thielemans K (1991) Treatment of murine B cell lymphoma with bispecific monoclonal antibodies (anti-idiotype x anti-CD3). J Immunol 147:1091–1097
33. Moreno MB, Titus JA, Cole MS, Tso JY, Le N, Paik CH, Bakacs T, Zacharchuk CM, Segal DM, Wunderlich JR (1995) Bispecific antibodies retarget murine T cell cytotoxicity against syngeneic breast cancer in vitro and in vivo. Cancer Immunol Immunother 40:182–190
34. Penna C, Dean PA, Nelson H (1994) Antitumor x anti-CD3 bifunctional antibodies redirect T-cells activated in vivo with staphylococcal enterotoxin B to neutralize pulmonary metastases. Cancer Res 54:2738–2743
35. Bakacs T, Lee J, Moreno MB, Zacharchuk CM, Cole MS, Tso JY, Paik CH, Ward JM, Segal DMA (1995)bispecific antibody prolongs survival in mice bearing lung metastases of syngeneic mammary adenocarcinoma. Int Immunol 7:947–955
36. Grosse-Hovest L, Brandl M, Dohlsten M, Kalland T, Wilmanns W, Jung G (1999) Tumor-growth inhibition with bispecific antibody fragments in a syngeneic mouse melanoma model: the role of targeted T-cell co-stimulation via CD28. Int J Cancer 80:138–144
37. Ruf P, Lindhofer H (2001) Induction of a long-lasting antitumor immunity by a trifunctional bispecific antibody. Blood 98:2526–2534